arXiv:astro-ph/0505526v1 26 May 2005

Discovery of X-ray Jets in the Microquasar H 1743−322.

S. Corbel[1], P. Kaaret[2], R.P. Fender[3], A.K. Tzioumis[4], J.A. Tomsick[5], J.A. Orosz[6]

ABSTRACT

We report on the formation and evolution of two large-scale, synchrotron-emitting jets from the black hole candidate H 1743−322 following its reactivation in 2003. In November 2003 after the end of its 2003 outburst, we noticed, in observations with the Australia Telescope Compact Array, the presence of a new and variable radio source about 4.6″ to the East of H 1743−322, that was later found to move away from H 1743−322. In February 2004, we detected a radio source to the West of H 1743−322, symmetrically placed relative to the Eastern jet. In 2004, follow-up X-ray observations with *Chandra* led to the discovery of X-ray emission associated with the two radio sources. This likely indicates that we are witnessing the interaction of relativistic jets from H 1743−322 with the interstellar medium causing in-situ particle acceleration. The spectral energy distribution of the jets during the decay phase is consistent with a classical synchrotron spectrum of a single electron distribution from radio up to X-rays, implying the production of very high energy (> 10 TeV) particles in those jets. We discuss the jet kinematics, highlighting the presence of a significantly relativistic flow in H 1743−322 almost a year after the ejection event.

Subject headings: black hole physics — radio continuum: stars — accretion, accretion disk — ISM: jets and outflows — stars: individual (H 1743−322, XTE J1550−564)

1. Introduction

Relativistic jets are now believed to be a common occurrence in black hole X-ray binaries (e.g. Corbel 2004, Fender 2004). The optically thin synchrotron spectra of the discrete ejection events (the so-called superluminal jets) imply that the emission becomes much fainter at higher frequencies. For that reason, such events were only observed at radio frequencies. However, Sams et al. (1996) reported the detection of extended infrared emission in GRS 1915+105 after a massive ejection event that could be of synchrotron nature. The most extreme case has been the detection of moving and decelerating X-ray (and radio) relativistic jets in the microquasar XTE J1550−564 a few years after the ejection event and on over large distances (Corbel et al. 2002; Tomsick et al. 2003a; Kaaret et al. 2003). The detection of optically thin synchrotron X-ray emission from discrete ejection events implies in-situ particle acceleration up to several TeV. This acceleration may be caused by interaction of the jets with the interstellar medium (ISM).

It now appears that relativistic jets emit throughout the entire electromagnetic spectrum. But are the jets of XTE J1550−564 unique due to special physical conditions or should we expect to observe similar X-ray jets in other X-ray Novae (XNe) ? If jets containing TeV particles are common amongst XNe, then there may be interesting consequences. The high energy parti-

[1]AIM - Unité Mixte de Recherche CEA - CNRS - Université Paris VII - UMR 7158, CEA Saclay, Service d'Astrophysique, F-91191 Gif sur Yvette, France.

[2]Department of Physics and Astronomy, University of Iowa, Iowa City, IA 52242 USA

[3] School of Physics and Astronomy, University of Southampton, Highfield, Southampton, SO17 1BJ, England

[4]Australia Telescope National Facility, CSIRO, P.O. Box 76, Epping NSW 1710, Australia.

[5]Center for Astrophysics and Space Sciences, University of California at San Diego, MS 0424, La Jolla, CA92093, USA.

[6] Department of Astronomy, San Diego State University, 5500 Campanile Drive, PA 210, San Diego, CA 92182-1221 USA

cles could produce a distinctive signature in the cosmic-ray flux (Heinz & Sunyaev 2002) or produce neutrinos if the jets contain protons (Distefano et al. 2002). Furthermore, the study of X-ray jets in microquasars could add an additional bridge between the physics of jets in microquasars and those from supermassive black holes. Interestingly, a connection with Gamma-Ray Burst has also been drawn by Wang, Dai & Lu (2003), who showed that the evolution of the eastern X-ray jet of XTE J1550−564 was consistent with the emission from adiabatically expanding ejecta heated by a reverse shock following its interaction with the ISM. The sensitivity of current X-ray missions (in particular *Chandra* and *XMM-Newton*) is sufficient to enable new discoveries in this emerging field and therefore provides further clues regarding the physical nature of these high energy phenomena.

H 1743−322 was discovered with Ariel 5 in August 1977 (Kaluzienski & Holt 1977) and has been precisely localized by HEAO-1 (Doxsey et al. 1977). It was originally proposed to be a black hole candidate (BHC) by White & Marshall (1983). H 1743−322 has probably been active several times during the past decades with activity observed in 1984 by EXOSAT (Reynolds et al. 1999) and in 1996 by TTM (Emelyanov et al. 2000). In March 2003, INTEGRAL detected new activity from IGR J17464−3213 (Revnivtsev et al. 2003) that was later found to correspond to H 1743−322. After its reactivation in 2003, a radio counterpart was found with the VLA by Rupen, Mioduszewski & Dhawan (2003a) and a bright radio flare (likely associated with a massive ejection event) was observed on 2003 April 8 (MJD 52738) by Rupen, Mioduszewski & Dhawan (2003b). During outburst, H 1743−322 went through several X-ray states with properties typical of BHC. Low and high frequency quasi-periodic oscillations have been detected in H 1743−322 by *RXTE* (Homan et al. 2005; Remillard et al. 2005). *Chandra* observations, during the 2003 outburst, revealed the presence of narrow and variable absorption lines in the X-ray spectrum of H 1743−322, possibly related to an ionized outflow (Miller et al. 2005). The 2003 active phase (as observed by RXTE/ASM) ended around late November 2003, but a new 4-month outburst started in July 2004 (Swank 2004) with a later reactivation at radio frequencies (Rupen, Mioduszewski & Dhawan 2004).

In this paper, we present an analysis of *Chandra* X-ray and ATCA radio observations of H 1743−322 from November 2003 through June 2004 that led to the discovery of large scale radio jets on each side of the BHC H 1743−322. More importantly, we also report the discovery of X-ray emission is very reminiscent of the large scale decelerating relativistic jets observed in XTE J1550−564 (Corbel et al. 2002). In §2, we describe the detection and localization of the radio and X-ray sources. In §3, we discuss the jet kinematics and the nature of the jet emission mechanism.

2. Observations and sources detection

2.1. Radio observations

Following the transition of H 1743−322 to the hard X-ray state (Tomsick & Kalemci 2003) on 2003 October 20 (MJD 52933), we initiated a series of radio observations with the Australia Telescope Compact Array (ATCA) starting on 2003 November 12 (MJD 52955). The ATCA synthesis telescope is located in Narrabri, New South Wales, Australia and consists of an east-west array with six 22 m antennas. A total of seven radio observations were carried out with the ATCA, mostly at 4800 MHz and 8640 MHz with occasional observations at 1384 MHz and 2496 MHz (see Tables 1 and 2 for details). The amplitude and band-pass calibrator was PKS 1934−638, and the antenna's gain and phase calibration, as well as the polarization leakage, were derived from regular observations of the nearby (5.8° away) calibrator PMN 1729−373. The editing, calibration, Fourier transformation, deconvolution, and image analysis were performed using the MIRIAD software package (Sault & Killen 1998).

No radio emission is detected at the position of H 1743−322 in any of our ATCA observations. However, we notice the presence of a new radio source (Fig. 1) about 4.6″ to the East of H 1743−322, immediately in the first ATCA observation. The following observations indicate that the new source increased in flux (see Tables 1 and 2 and Fig. 2). The position of the source also changed over time, moving away from the BHC H 1743−322. We discuss the motion of the source

Table 1: Radio Observations of H 1743−322 and associated jets: position and angular separation.

Date	MJD	Source	Position		Angular
			R.A.	Decl.	Separation
2003/11/12	52955.86	Eastern Jet	17 46 15.978	-32 14 01.08	$4.63 \pm 0.30''$
2003/11/30	52973.72	Eastern Jet	17 46 15.995	-32 14 00.15	$4.91 \pm 0.30''$
2003/12/09	52983.45	Eastern Jet	17 46 16.005	-32 14 00.83	$4.98 \pm 0.30''$
2003/12/20	52994.49	Eastern Jet	17 46 16.026	-32 14 00.67	$5.25 \pm 0.30''$
2004/02/13	53049.40	Eastern Jet	17 46 16.056	-32 14 00.40	$5.65 \pm 0.50''$
		Western Jet	17 46 15.274	-32 14 00.78	$4.30 \pm 1.00''$
2004/04/07	53103.22	No detection			
2004/06/01	53158.15	No detection			

MJD: Modified Julian Date (observation midtime). The angular separation is based on the *Chandra* position of the black hole H 1743−322.

Table 2: Radio Observations of H 1743−322 and associated jets: flux density and spectral index.

Date	MJD	Source	Flux density (mJy) MHz				Spectral index
			1384	2368	4800	8640	
2003/11/12	52955.86	Eastern Jet	...	...	1.10 ± 0.10	0.48 ± 0.11	-1.41 ± 0.42
2003/11/30	52973.72	Eastern Jet	...	...	1.55 ± 0.09	0.87 ± 0.09	-0.98 ± 0.20
2003/12/09	52983.45	Eastern Jet	...	...	1.86 ± 0.09	0.84 ± 0.09	-1.35 ± 0.20
2003/12/20	52994.49	Eastern Jet	...	...	2.37 ± 0.06	1.34 ± 0.07	-0.97 ± 0.10
2004/02/13	53049.40	Eastern Jet	0.62 ± 0.15	0.41 ± 0.15	0.33 ± 0.05	< 0.21	-0.49 ± 0.22
		Western Jet	< 0.45	< 0.45	0.14 ± 0.05	< 0.21	N.A.
2004/04/07	53103.22	Eastern Jet	...	...	< 0.18	...	N.A.
2004/06/01	53158.15	Eastern Jet	< 0.45	< 0.30	< 0.12	...	N.A.

MJD: Modified Julian Date (observation midtime). Radio upper limits are given at the 3 sigma level. Fluxes for the western jet are only given for the day of its unique ATCA detection, otherwise the upper limits can be deduced from the error bars (one sigma) or upper limits on the flux densities of the eastern jet.

in a later section taking into account the additional constraints from the *Chandra* observations.

The light-curve of this source, combining all our ATCA observations (at 4800 MHz and 8640 MHz), is presented in Figure 2. This source was brightening from our first observations until the end of 2003. The single detection on 2004 February 13 (MJD 53049) at a much (almost a factor ten) fainter level points to a very fast decay. The maximum of radio emission was likely in January 2004. The rise of radio emission at 4800 MHz is gradual, whereas there may be some variations during the rise at 8640 MHz. We fitted an exponential rise and a power-law rise to the radio data (at both frequencies) and found that both fits are equally acceptable. The time-scales are consistent for both radio frequencies. The $1/e$-folding time of the exponential rise is 49.4 ± 4.8 days at 4800 MHz and 40.0 ± 6.8 days at 8640 MHz. The index of the power-law rise is 4.9 ± 0.5 at 4800 MHz and 6.0 ± 1.0 at 8640 MHz.

Due to the fast decay of radio emission, we can not accurately constrain its decay rate. However, we can give some limits that clearly indicate that the decay is faster than the rise. Assuming a maximum at the time when we detected the source at its brightest level (on 2003 December 20), and taking the 4800 MHz detection during the decay, we deduced an $1/e$-folding time of the exponential decay of 27.9 ± 2.2 days or an index of the power-law decay of 10.2 ± 0.8. We emphasize that these limits (an upper limit on the $1/e$-folding time and a lower limit on the index of the power-law) are quite conservative and that the true decay during

the early part of 2004 is likely faster than indicated by these numbers. The light-curve at 8640 MHz is consistent with that at 4800 MHz, but very few data points are available.

We searched for linearly polarized radio emission when the eastern source was at its brightest level (i.e. on 20 December 2003). Linear polarization at the level of 9.9 ± 2.9% with a mean polarization angle of 51.9 ± 8.3° is detected at 4800 MHz. At 8640 MHz, we find an (3 sigma) upper limit of ∼ 21% on the polarization. This limit is weak because the 8640 MHz flux density is weaker than at 4800 MHz.

In addition to the new source to the East of H 1743−322, we note that a radio source is detected to the West of H 1743−322 (Figure 3), almost symmetrically placed relative to the Eastern source, only on 2004 February 13 with a flux density of 0.14 ± 0.05 mJy at 4800 MHz. Despite its weak flux density, the *Chandra* data on the same day (Figs. 4 and 5) confirm the existence of an X-ray source at this position and therefore strengthen the reality of the western radio source.

As both of these radio sources appear to be moving away from the BHC, we conclude that they are related to the H 1743−322 system. The properties are very reminiscent to the large scale relativistic radio and X-ray jets of XTE J1550−564 (Corbel et al. 2002) after 2000. It is therefore likely that these evolving radio sources represent the action of previously ejected plasma on the ISM. As discussed below, the most likely ejection date is around 2003 April 8 when a major radio flare was observed by Rupen et al. (2003). We will now refer to these sources as the eastern and western jets, based on their location with respect to H 1743−322. We report in Tables 1 and 2 their positions (from radio observations), angular separation from H 1743−322, as well as their flux densities. As H 1743−322 is not detected at radio frequencies, we used its *Chandra* position as defined in the next section.

2.2. X-ray observations

2.2.1. Source detection

Following the detection of the eastern moving radio source and its strong similarities with the large scale X-ray jets in XTE J1550−564 (Corbel et al. 2002; Tomsick et al. 2003a; Kaaret et al. 2003), we triggered our target of opportunity proposal for the *Chandra X-ray Observatory* (Weisskopf et al. 2002) to search for an X-ray counterpart to the radio jets. The *Chandra* observations were significantly delayed relative to the trigger because H 1743−322 passed near the Sun and was not observable. As indicated previously, the eastern jet was already decaying when the *Chandra* observations were performed (see Fig. 2 for their scheduling relative to the radio light-curve).

H 1743−322 was observed with *Chandra* on 2004 February 12 (MJD 53048), March 24 (MJD 53089) and March 27 (MJD 53092) using the Advanced CCD Imaging Spectrometer spectroscopic array (ACIS-S; Bautz et al. 1998). In all observations, the target was placed on one of the back-illuminated ACIS Chips (S3) with the ACIS-S operated in imaging mode. For the first observation, only the S3 chip was read out and a 1/2 sub-array mode was used to limit pile-up. For the latter two observations, the source was known to be a lower flux state and the full ACIS-S imaging mode array was used.

We produced 0.3–8 keV ACIS images using the "level 2" event lists from the standard data processing (ASCDS v7.2.1) using the *Chandra* Interactive Analysis of Observations (CIAO) software package version 3.0.2 and Calibration Data Base (CALDB) version 2.26. We constructed light curves with all valid events on the S3 chips to search for time of high background. Only weak background flares were found (and removed) for the February observation, otherwise the count rate appears uniform. The total useful exposure obtained was 17796 s on February 12 (Obs. 1), 28363 s on March 24 (Obs. 2), and 40037 s on March 27 (Obs. 3).

We searched for X-ray sources in each 0.3–8 keV image using *wavdetect* (Freeman et al. 2002), the wavelet-based source detection routine in CIAO. For all three *Chandra* observations, an X-ray source is found at the location of H 1743−322, the eastern jet, and western jet (Figs 4 and 5). All three sources appear aligned and therefore provide further evidence for a connection with H 1743−322.

We check the *Chandra wavdetect* position of each source by calculating the source's centroid using the 0.3-8 keV events from a 4 × 4 pixels ($2''\times 2''$) region centered on the it wavdetect positions.

This region contains all events likely related to the source along with a small number of background events. The recalculated positions of H 1743−322, the eastern and western jets were in good agreement with the *wavdetect* positions; the differences were less than 0″.10. The position angle of the eastern jet relative to H 1743−322 is 89.0 ± 1.5 °, while the position angle of the western jet is –91.7 ± 1.8 °.

2.2.2. Source localization

To obtain the best constraint on the position of each detected source (especially H 1743−322, which is not detected in our radio images), we registered the *Chandra* images with an infrared image from the 2 Micron All-Sky Survey (2MASS) following the procedure described in Tomsick et al. (2003b). We use the two longest *Chandra* observations (# 2 and 3) and inspected each observation separately. We restricted our search for X-ray and infrared sources within a 4 arcmin radius circle centered on the position of H 1743−322 as reported by *wavdetect*.

We cross-correlated the *Chandra* source positions with the 2MASS sources in the field. We find that 5 *Chandra* sources have 2MASS sources within the *Chandra* pointing uncertainty of 0″.6 for observation 2 and 9 for observation 3. The accuracy of the 2MASS source positions is 0″.2 (90% confidence). For these sources, the angular separation between the 2MASS and *Chandra* positions ranges from 0″.07 to 0″.22 for observation 2 and from 0″.06 to 0″.46 for observation 3. Given the surface density of 2MASS sources, there is a 0.11% probability that a match with the largest separation is spurious for observation 2, and 0.50% for observation 3. We used the full set of matches to register each X-ray image. The average 2MASS to *Chandra* differences are $-0''.01 \pm 0''.11$ in R.A. and $-0''.05 \pm 0''.10$ in Decl. for observation 2 and $-0''.19 \pm 0''.10$ in R.A. and and $-0''.09 \pm 0''.08$ for observation 3. We estimated the location of H 1743−322 as the average of the positions measured in the two *Chandra* images after registration to the 2MASS positions by performing the above indicated shifts. H 1743−322 is found to be located at R.A. = 17h 46m 15.s613, Decl. = −32° 14′ 0″.95 with a total uncertainty of 0.″10 (including the 0.2″ systematics due to the registration to 2MASS images and the statistical uncertainties on the *Chandra* *wavdetect* position). The difference in position of the eastern and western jets, after the registering process, between the two *Chandra* observations (only separated by 2.5 days) were less than 0.″10 (i.e. within the total uncertainty). This precise *Chandra* position of H 1743−322 is consistent within uncertainties (a difference of 0.25″) with the recently refined VLA radio position (Rupen, Mioduszewski, & Dhawan 2004).

We used the position of H 1743−322 to register *Chandra* observation # 1 on the 2MASS frame, for which shifts of -0.25 ± 0.17 arcsecond (in R.A.) and -0.32 ± 0.16 arcsecond (in Decl.) are needed. These shifts are smaller than the *Chandra* absolute astrometric of 0.6″ at 90% confidence. We report in Table 3 the location of H 1743−322 , the western and eastern jets, as well as the angular separation between the jets and the BHC for all three *Chandra* observations. We note that the angular separation does not depend on the image registration.

2.2.3. Flux and energy spectra

We extracted an energy spectrum in the 0.3–8 keV energy range for the eastern and western jets in all three *Chandra* observations using CIAO v3.0.2 tools and we fitted these spectra using XSPEC v11.3.0. We used a circular source extraction region with a radius of 2.3″, resp. 1.2″, and we extracted background spectra from an annulus with an inner radius of 13″ and an outer radius of 22″, resp. 19.5″ for the eastern and western jets respectively. These regions were centered on the jet positions as given by *wavdetect*. Due to the low numbers of source counts (at maximum of 24 counts), we used the W statistic for fitting (Wachter, Leach & Kellog 1979; Arnaud, in prep.) the un-binned spectra, this is adapted from the Cash statistic (Cash 1979) and works with background subtracted spectra and low count rate.

These spectra are adequately fitted with a power-law model including interstellar absorption. We fixed the equivalent hydrogen absorption column density, N_H, to the constant value measured in *Chandra* observations of H 1743−322 during its 2003 outburst (Miller et al. 2005), i.e. 2.3×10^{22} cm^{-2}. For the eastern jet, the best-fit photon index is 1.67 ± 0.90, 1.78 ± 1.10 and 2.03 ± 0.90 for *Chandra* observations # 1, 2 and 3 respectively.

Table 3: *Chandra* Observations of H 1743−322.

Obs.	Date	MJD	Exposure	Source	Position			Angular
#	2004-		time (s)		R.A.	Decl.	Uncertainty	Separation
1	02-12	53048.0	17796	H 1743−322	17 46 15.613	-32 14 0.95	0.10″	N.A.
				Eastern Jet	17 46 16.094	-32 14 0.92	0.19″	6.10 ± 0.20 ″
				Western Jet	17 46 15.263	-32 14 1.44	0.24″	4.47 ± 0.30 ″
2	03-24	53088.9	28363	H 1743−322		See Obs. # 1		N.A.
				Eastern Jet	17 46 16.142	-32 14 0.76	0.17″	6.72 ± 0.20 ″
				Western Jet	17 46 15.243	-32 14 1.05	0.16″	4.70 ± 0.20 ″
3	03-27	53091.5	40037	H 1743−322		See Obs. # 1		N.A.
				Eastern Jet	17 46 16.135	-32 14 0.83	0.11″	6.63 ± 0.20 ″
				Western Jet	17 46 15.243	-32 14 1.09	0.15″	4.70 ± 0.20 ″

MJD: Modified Julian Date (exposure midtime). The angular separation between the jets and H 1743−322 is based on the *Chandra* position of the black hole H 1743−322 as estimated in observation # 2 and 3 during the 2MASS/*Chandra* registration process. The uncertainties on the position include systematics due to the registration process and the statistical uncertainties on the *wavdetect* position. However, the angular separation does not depend on the image registration.

Refitting these three datasets simultaneously (allowing the normalization to vary) led to a photon index of 1.83 ± 0.54 (with 90% confidence errors). We did the same for the western jet, giving photon indexes of 2.5 ± 2.5, 2.2 ± 1.0 and 1.6 ± 1.0 for *Chandra* observations # 1, 2 and 3 respectively and a photon index of 1.9 ± 0.8 (with 90% confidence errors) for the combined spectrum.

We fixed the power-law photon index (see section 3.2.2) to a value of 1.6 to obtain measurements of the X-ray flux. This value is extracted from the fit to the radio/X-ray spectral energy distribution. We measure 0.3–8 keV absorbed fluxes for the eastern jet of (21.3 ± 4.9) × 10^{-15}, (10.0 ± 2.6) × 10^{-15}, and (9.4 ± 2.3) × 10^{-15} ergs s^{-1} cm^{-2} for observations 1, 2, and 3, respectively. Concerning the western jet, the 0.3–8 keV absorbed fluxes are (3.0 ± 2.1) × 10^{-15}, (6.4 ± 2.6) × 10^{-15}, and (6.2 ± 1.8) × 10^{-15} ergs s^{-1} cm^{-2} for observations 1, 2, and 3, respectively. The unabsorbed fluxes, in the same band, are 2.0 higher than the absorbed values quoted above. The quoted errors are based on the numbers of source and background counts and Poisson statistics.

Figure 6 shows the time variation of the 0.3–8 keV unabsorbed flux of the eastern and western jets. The X-ray emission of the eastern jet is decaying, whereas the emission from the western jet is consistent with a slightly rising source (or even constant). We fitted an exponential or a power-law decay to the eastern jet and we found that both fits are equally acceptable. The $1/e$-folding time of the exponential decay is 53.5 ± 19.6 days, whereas the index of the power-law decay is 6.2 ± 2.3. The constraints are rather weak for the western jet, the $1/e$-folding time of the exponential rise is 58.2 ± 46.3 days and the index of the power-law rise is 5.7 ± 4.5.

We note that the western jet was likely detected at 4.8 GHz during the first *Chandra* observation (Figure 3), but unfortunately no radio observation was possible during the time of the second and third *Chandra* observations. However, we did perform a ATCA observation about 2 weeks after the third *Chandra* observations but failed to detect radio emission from the western jet (with similar sensitivity to its detection in February, see Table 2). This indicates that the peak of emission from the western jet was likely sometime between February and the beginning of April 2004, i.e. roughly 2 or 3 months after the peak of emission from the eastern jet. At this peak, the X-ray (0.3 – 8 keV band) luminosity (for a distance of 8 kpc) of the eastern jet was of the order of more than 3 × 10^{32} ergs s^{-1}, i.e. a level consistent with the X-ray emission of some BHCs while in their quiescent state (e.g. Garcia et al. 2001). Therefore, if the production of X-ray jets is more common than previously thought as we suggest here, some of the reported measurements of the quiescent X-ray emission of BHC may be contaminated by jet emission, particularly for observations made using instruments with worse angular resolution than *Chandra*.

2.2.4. Source morphology

The western jet of XTE J1550−564 was clearly extended with a leading peak and a trailing tail extended up to 5″ toward the black hole (Kaaret et al. 2003). To study the morphology of the X-ray jets in H 1743−322, we decomposed the images along axes parallel and perpendicular to the jet axis defined as a line extending through the black hole candidate and the jets. Following the procedure described in Kaaret et al. (2003), we calculated the displacement of each X-ray event parallel and perpendicular to this axis. All photons with energies in the range 0.3–8 keV and within 2″ of the jet axis in the perpendicular direction are included. For each observation, we compared the morphology of the black hole candidate H 1743−322, assumed to be point-like, to each of the detected jets, except for observation 1 in which the Western jet had too few counts for a meaningful comparison.

We carried out the morphology comparison using a Kolmogorov-Smirnov (KS) test to permit comparison of unbinned position data. We shifted the jet positions to match the black hole candidate position using the positions derived from *wavdetect*. We compared the morphology for events lying with 2″ along the jet axis of each source position. We find no significant evidence for spatial extent along or perpendicular to the jet axis for any jet in any observation. We also combined the data from observations 2 and 3 (Fig. 7) and still did not find any significant evidence for spatial extent of either jet. The KS-test probabilities that the black hole and jet samples are drawn from the same parent distribution range from 0.11 to 0.96. To place an upper bound on the size of the Western jet along the jet axis, we calculated the standard deviation of the displacements of events along the jet axis from the *wavdetect* position of the jet. We find a value of $0.61 \pm 0.04''$. This is inconsistent with the standard deviation calculated for the black hole candidate ($0.48 \pm 0.02''$) by only 2.7σ, so, again, there is no strong evidence for spatial extent and the value should be taken as an upper limit on the jet size.

In order to increase the statistics for the comparison source, we decided to compare the X-ray jet profiles to the profiles for the source PG 1634+706 (observation ID 1269), which is used to calibrate the ACIS point-spread function. Again, the KS test does not indicate significantly that the BHC H 1743−322 or its associated X-ray jets are extended along or perpendicular to the jet axis.

3. Discussion

3.1. Proper motion and jet kinematics

The positions of the eastern and western jets change between the various radio and X-ray observations with the jets are moving away from the BHC H 1743−322. In order to quantify this motion, we have calculated the angular separation between H 1743−322 and each jet. For all *Chandra* and ATCA observations, we used the position of H 1743−322 as determined in the previous section. Figure 8 shows the angular separation between H 1743−322 and each jet as a function of time. In this figure, the origin of time (day 0) is the day (2003 April 8 = MJD 52738) in which a major radio flare, and hence a massive plasma ejection, was observed (Rupen et al. 2003b).

This figure clearly illustrates that the eastern jet is moving away from H 1743−322. The *Chandra* and ATCA positions of the eastern jet are consistent with a linear increase of the angular separation versus time and a linear fit to the angular separation implies a proper motion of 15.2 ± 1.8 mas day^{-1}. The *Chandra* locations are consistent with a continuation of the motion from the ATCA observations. The data for the western jet are only weakly inconsistent with a fixed position. A linear fit to the angular separation for the western jet gives a proper motion of 6.7 ± 5.2 mas day^{-1}.

Extrapolation of the linear fit for the eastern jet (for which we have the best statistics) implies zero separation on MJD 52652 ± 38 (i.e. around 2003 January 13). This date is well before the initial detection of H 1743−322 by INTEGRAL on 2003 March 21 (MJD 52719; Revnivtsev et al. 2003). With the RXTE/ASM data, it is not possible to assess the X-ray activity of H 1743−322 around MJD 52652. However, observations of several black hole systems (Corbel et al. 2004; Fender et al. 2004) has revealed that the massive ejection events occurred later the during the outburst at a period consistent with the transition from the intermediate state to the steep power-law state. Again, the bright radio flare observed by Rupen

et al. (2003b) on 2003 April 8 (MJD 52737) is consistent with this interpretation, as illustrated by e.g. the hardness evolution of the X-ray spectra (Capitanio et al. 2005).

For the rest of this paper, we therefore consider the time origin of the jets as the day of the bright radio flare (day zero in Figure 8). With the linear fit to the motion of the eastern jet, we predict an angular separation of 1.29 ± 0.55 ″ at the time of the first bright radio flare. If the velocity of the eastern jet was constant, we should have obtained a zero separation on this day. Whereas the deviation from zero is not highly significant (2.4 sigma or 98% confidence level), this could imply that the jets were intrinsically more relativistic at the time of ejection and decelerated gradually later on. This would be another similarity with the X-ray jets of XTE J1550−564 (Corbel et al. 2002). More frequent radio and/or X-ray observations would have been necessary to better constrain this motion.

The proper motion of the eastern jet appears higher that of the western jet. Also, the X-ray flux of the western jet continues to rise and the eastern jet is decaying in both the radio and X-rays. The western jet is not detected at radio frequency during the April and June 2004 ATCA observations, despite a sensitivity similar to the February 2004 observation (Table 2). This could suggest that the rise of emission from the western jet has stopped and that the peak of its emission occurred sometimes between February and April 2004, i.e. few months after the peak observed for the eastern jet. This probably indicates that the eastern jet is approaching and the western jet is receding.

3.1.1. Case of ballistic jets

As there is no strong indication of a decelerating jet in H 1743−322 , we first consider the kinematics of the jets under the assumption of an intrinsically symmetric ballistic ejection (e.g. see Fender et al. 1999 for the formalism). From the first detection of the jets (ATCA on MJD 52956 for the eastern jet and *Chandra* on MJD 53092 for the western jet), we estimate their average proper motions between ejection on 2003 April 8 and their first detections. We deduced an average proper motion of 21.2 ± 1.4 mas day^{-1} for the eastern jet and 13.3 ± 0.6 mas day^{-1} for the western jet. From this, we derive $\beta cos\theta = 0.23 \pm 0.05$, with $\beta = v/c$ the true bulk velocity and θ the angle between the axis of the jet and the line of sight. This immediately gives a maximum angle to the axis of the jets of $\theta_{max} \leq 77 \pm 3°$ and a minimum velocity of $\beta_{min} \geq 0.23 \pm 0.05$. We can also infer a maximum distance to H 1743−322 of 10.4 ± 2.9 kpc. To date, the distance to H 1743−322 is basically unknown, however its location toward the Galactic bulge could possibly imply a Galactic Center location, which would be consistent with the above upper limit. If we assume a source distance of 8 kpc (distance to the Galactic center), we derive an intrinsic velocity of the ejection of $\beta = 0.79$ and an angle of $\theta = 73°$ for the axis of the jets. At this distance the apparent velocity of the eastern jet ($\beta_{app} = v_{app}/c$) is 0.98 and for the western jet we deduce an apparent velocity ($\beta_{rec} = v_{rec}/c$) of 0.61. This clearly indicates the presence of a significantly relativistic outflow in H 1743−322 , almost a year after the ejection event.

3.1.2. Case of decelerating jets

If the jets have been gradually decelerated since the ejection event, the average proper motions can not be used to constrain the jets kinematics. In that case, we can still study their properties using the 2004 measurements of the proper motions (15.2 ± 1.8 mas day^{-1} for the eastern jet and 6.7 ± 5.2 mas day^{-1} for the western jet). We again assume a source distance of 8 kpc, keeping in mind that this is a major source of uncertainty in the derived parameters. At this distance the apparent velocity of the eastern jet ($\beta_{app} = v_{app}/c$) is 0.71 ± 0.08 and for the western jet we deduce an apparent velocity ($\beta_{rec} = v_{rec}/c$) of 0.31 ± 0.24. The true bulk velocity, $\beta = v/c$, is defined as $\beta = \beta_{app}/(\beta_{app}\cos\theta + \sin\theta)$, with θ equal to the angle between the axis of the jet and the line of sight. This function has a minimum at $\theta_{min} = \tan^{-1}(1/\beta_{app}) = 54°$ with our measured apparent velocity for the approaching jet (again for a distance of 8 kpc). This translates into a minimum true bulk velocity of $\beta_{min} = 0.57 \pm 0.05$, still indicating the presence in 2004 of a significantly relativistic flow in H 1743−322.

3.2. Flux evolution and emission mechanism

3.2.1. Radio emission: Spectra

We define the radio flux density $S_\nu \propto \nu^\alpha$, with α the radio spectral index and ν the frequency. We note a difference in the properties of radio emission during the rise versus decay and the decay phases. The radio spectra are consistent with being optically thin (i.e. $\alpha \leq 0$) all the time. We note that the spectra are very steep during the rise (see Table 2, $|\alpha| \geq 1$), whereas the single radio detection during the decay is more typical of optically thin synchrotron emission ($\alpha = -0.49 \pm 0.22$). The detection of a significant level of polarization (when the sensitivity allowed it) is consistent with the radio emission being optically thin synchrotron emission. The broadband spectra (see below) accurately constrains the spectral index and is consistent with a classical synchrotron spectral index of $\alpha \sim -0.6$. This index from the broadband SED on 2004 February 12-13 is significantly different from the average radio spectral index during the rise, which is $\alpha = -1.18 \pm 0.13$.

The difference of spectral indices during the rise is probably not related to the emission beeing resolved out at high frequency by the ATCA, as the four radio observations during the rise were performed in various configurations of the telescope. In addition, we note that both jets are not resolved by *Chandra*, and therefore they should appear as point sources to ATCA. Whereas the synchrotron slope is almost a textbook example during the decay, the spectral index during the rise is likely an intrinsic property of the process that accelerates the emitting particles during the collision of relativistic plasma with the local medium. This may possibly be explained as followed: The rising phase represents the propagation of the jets through a dense medium associated with a mechanism that accelerate particles to high energy, whereas the decaying phase represents propagation through a less dense medium and possibly without any further re-acceleration of particles in the jets. The emission properties during the decay phase would then be governed by synchrotron and/or adiabatic losses of the relativistic particles. The steep spectrum during the rise may eventually shed light on the mechanism that accelerates particles to high energies.

3.2.2. Broadband spectra and emission mechanism

The eastern and western jets are simultaneously detected at radio and X-ray frequencies on 2004 February 12-13. Figure 9 shows the broadband spectral energy distribution of the jets at this epoch. The radio fluxes are from Table 2, and we convert the unabsorbed 0.3–8 keV flux to a flux density at a pivot X-ray energy defined by allowing the X-ray photon index to vary (Fig. 9). A combined fit of the radio and X-ray data result in a spectral index of -0.64 ± 0.02, which is typical of synchrotron emission. The same is true for the western jet, giving a radio/X-ray spectral index of -0.70 ± 0.05 on 2004 February 12-13.

The detection of linear polarization ($\sim 10\%$) from the eastern jets of H 1743−322, as well as the spectral index, strongly favor synchrotron emission as the physical origin of the radio emission in the jets. The fact that the X-ray emission is consistent with an extrapolation of the radio power-law suggests that the synchrotron emission extends up to X-rays.

We can therefore derive the minimum energy associated with the eastern jet on 2004 February 12-13 (the jet for which we have the best constraints) under the assumption of equipartition between the magnetic and electron energy densities (Longair 1994). We assume the case of ballistic ejection (section 3.1.1), corresponding to an angle between the jet axis and the line of sight of $\theta = 73^\circ$ and a bulk velocity $\beta = 0.79$. We use a frequency range of 1.4×10^9 Hz to 2×10^{18} Hz with a spectral index of –0.6 and a flux density of 2.4 nJy at the pivot energy (Figure 9) of 2.7 keV.

The major uncertainty for this calculation is the estimate of the volume of the emitting region. For that purpose, we use the same method as in Tomsick et al. (2003a) by assuming that the emitting region is a section of a cone with its vertex at the compact object. An upper limit can be obtained using the *Chandra* constraint on the source size (FWHM $\leq 1.4''$) as calculated in section 2.2.4. The opening angle of the cone is not well constrained, so we consider the upper limit from the *Chandra* observations of 12° and also 1° as in XTE J1550−564 (Kaaret et al. 2003), giving a volume of the emitting region of about 4×10^{51} cm^3 (for an opening angle of 12°) or 3×10^{49} cm^3

(for 1°).

For this volume range, the corresponding minimum energy required is about 1.6 $\times 10^{42}$ to 1.4 $\times 10^{43}$ erg and the associated magnetic field for which the energy in relativistic particles equals the magnetic energy is in the range 0.2 to 0.8 mG. The kinetic energy of a pure electron/positron plasma is 10^{42} to 9 $\times 10^{42}$ erg. If there is one proton per electron, then the kinetic energy of the electron/proton plasma is about 2 $\times 10^{42}$ to 1.1 $\times 10^{43}$ erg. The associated mass of this electron/proton plasma would be of the order of 10^{21} to 4 $\times 10^{21}$ g. For a typical mass accretion rate of 10^{18} g s^{-1}, this amount of material could be accumulated in 1000 to 4000 s. As the mass outflow rate is likely much lower, an accumulation time of the order of a day would be obtained if we assume a few percents efficiency, this could be consistent with the timescale of the initial radio flare.

The Lorentz factor of the X-ray synchrotron emitting electrons would then be of the order of 1 to 3 $\times 10^7$ (taking a pivot energy of 2.7 keV and assuming equipartition), giving synchrotron lifetime cooling of the orders of 2 to 50 years, i.e. much longer than the lifetime of the X-rays jets of H 1743−322. It is interesting to note (keeping in mind the limitation on the volume estimate) that all the above derived quantities are of the same order of magnitude as those derived for XTE J1550−564 (Corbel et al. 2002; Tomsick et al. 2003a; Kaaret et al. 2003).

In the above, the X-ray emission seems consistent with an extrapolation of the synchrotron radio spectrum. However, it is of some interest to see if some other emission mechanism, such as inverse Compton or synchrotron self-Compton, could also be viable at high energy. Assuming that only the radio emission is of synchrotron origin lead to an equipartition magnetic field of 0.2 to 0.7 mGauss; from this we deduce a range for the magnetic energy density of the order of 2 $\times 10^{-9}$ to 2 $\times 10^{-8}$ erg cm^{-3}. The synchrotron photon energy density is then estimated, similarly to the XTE J1550−564 case (Tomsick et al. 2003a), to be of the order of 6 $\times 10^{-17}$ to 2 $\times 10^{-15}$ erg cm^{-3}. The synchrotron photon density is well below the magnetic energy density, implying that SSC is very likely not important at X-ray frequencies. As argued in Tomsick et al. (2003a), inverse-Compton emission from the interstellar radiation field and the cosmic microwave background are unlikely because the associated energy density is well below the magnetic energy density. All of these considerations point to a coherent picture which is that the X-ray emission associated with the jets of H 1743−322 is synchrotron emission and therefore very high energy (> 10 TeV) particles are produced in those jets.

3.3. A comparison with other X-ray jets

With this discovery of transient X-ray jets in H 1743−322, we can now come to the idea that such events may be a common occurrence associated with any X-ray binary in outburst. Indeed, after the original discovery of X-ray jets in XTE J1550−564 (Corbel et al. 2002), a relativistic ejection in GX 339−4 has also been observed to later develop into a large scale jet, possibly related to the interaction with the ISM (Gallo et al. 2004). However, the western large scale jet of GX 339−4 has only been observed at radio frequencies (E. Gallo, private communication), possibly due its fast decay rate. Indeed, taking the radio flux density quoted in Gallo et al. (2004), we can estimate the time-scale associated to the two knots in the large scale jets of GX 339−4 assuming an exponential or a power-law decay. The $1/e$-folding times of the exponential decays are 47.3 ± 8.3 days and 57.0 ± 14.7 days, whereas the indeces of the power-law decays are 5.9 ± 1.0 and 4.9 ± 1.0, respectively for knot A and knot B. These timescales are consistent with those of H 1743−322, but much faster than those of XTE J1550−564 (Kaaret et al. 2003). The X-ray observation of GX 339−4 was 6 months after the last detection of the western large scale jet at radio frequencies (Gallo et al. 2004) and any X-ray emission likely decayed away before the observation.

It is unclear why the decay could be faster in some sources, but this may be related to local ISM conditions. Also, as outlined by Wang et al. (2003), the (already) fast decay of the X-ray emission from the eastern X-ray jet in XTE J1550−564 was not consistent with a forward shock propagating through the ISM. On the contrary, if the emission was driven by a reverse shock following the interaction of the ejecta with the ISM, then the rapidly fading X-ray emission could be the synchrotron emission from adiabatically expanding ejecta. With a "much" faster decay in H 1743−322 or even GX 339−4, it may also be possible that

the emission in these two cases is also related to a reverse shock moving back into the ejecta. In that case, it would be interested to see if a reverse shock model (as in Wang et al. 2003) could also reproduce the flux and spectral evolution that we observed during the rise of emission of the jets of H 1743−322. Also the fast transition between the rising and fading phases should also be explained.

In addition, we would like to mention the strong similarities with the neutron star system Sco X–1, which shows the ballistic motion of two radio lobes located on each side of the compact star (Fomalont et al. 2001a,b). However, the Sco X–1 lobes are powered by a continuous and unseen ultra relativistic beam of energy (Fomalont et al. 2001a,b), possibly related to the fact that Sco X–1 is always close to the Eddington luminosity for a neutron star. Similarly, as discussed before, the bright radio flare in H 1743−322 on 2003 April 8 took place around the transition to a steep power-law state, i.e. the state which is believed to be close to the Eddington luminosity. Otherwise, H 1743−322, like most X-ray transients, is usually believed to be in a state of low accretion rate (quiescence), and even if a large fraction of the accretion energy could be carried out by an outflow (compact jet) in this accretion regime (Fender 2004), the total amount of energy would still be much less than in the brighter X-ray state. Therefore, as we do not have any indication for a continuous and persistent powerful beam of energy in H 1743−322, we believe that the evolution of the large scale jets in H 1743−322 and XTE J1550−564 is the result of one (or several in a short period) inpulsive ejection event(s) which later interact with the ISM.

As we have calculated above, many of the parameters (magnetic field, particle energy, etc.) derived for H 1743−322 are consistent with those obtained for XTE J1550−564, and therefore strengthen the similarities between these two sources. Here, we point to another similarity. When first detected, both jets in H 1743−322 were at the same angular distance ($\sim$ 4 arcsec = 0.16 pc for a distance of 8 kpc) from the black hole (however, we note that the eastern jets may have been active some time before our first ATCA observations), i.e. the plasma originally ejected (probably around 2003 April 8) by the black hole has traveled the same distance before brightening again, possibly due to the collision with denser ISM. Similarly, in XTE J1550−564 the jets were observed to brighten at the same angular distance ($\sim$ 22 arcsec = 0.5 pc for a distance of 5.3 kpc) from the black hole. This could indicate that these two black holes lie in a cavity or that the jets propagate through an evacuated channel pre-existing to the outburst (e.g. Heinz 2002) and that they "turn on" again when they hit a denser ISM phase.

Whereas either the ejection or the ISM was not symmetric or homegeneous in the case of XTE J1550−564 (Kaaret et al. 2003), the evolution of the radio emission of both jets may also suggest a similar case in H 1743−322. Indeed, on 2004 February 13, the western jet was at an angular separation of 4.47 ± 0.30 $''$ and with the kinematics of the jets as outlined previously, it should have passed through the 4.63 to 5.25 arcsecond region during the last two radio observations. If the ejection was symmetric and the ISM homegeneous, the western jet should have been brighter at radio frequencies in April-June than in February 2004. The non-detection of the western jet in the last two ATCA observation may therefore suggest a hint of asymmetry in the ISM density or in the ejection. However, a more detailled lightcurve would have been necessary to confirm this.

The Australia Telescope is funded by the Commonwealth of Australia for operation as a national Facility managed by CSIRO. *RXTE*/ASM results are provided by XTE/ASM team at MIT. This publication makes use of data products from the Two Micron All Sky Survey, which is a joint project of the University of Massachusetts and the Infrared Processing and Analysis Center/California Institute of Technology, funded by the National Aeronautics and Space Administration and the National Science Foundation. We thank the referee for constructive comments. SC acknowledges useful discussions with S. Heinz. PK acknowledges partial support from NASA Chandra grant GO4-5039X. JAT acknowledges partial support from NASA Chandra grant GO3-4040X.

REFERENCES

Bautz, M. W., et al. 1998, Proc. SPIE, 3444, 210

Capitanio, F., et al. 2005, ApJ, 622, 503

Cash, W. 1979, ApJ, 228, 939

Corbel, S., Fender, R. P., Tzioumis, A. K., Tomsick, J. A., Orosz, J. A., Miller, J. M., Wijnands, R., & Kaaret, P. 2002, Science, 298, 196

Corbel, S., Fender, R. P., Tomsick, J. A., Tzioumis, A. K., & Tingay, S. 2004, ApJ, 617, 1272

Corbel, S. 2004, AIP Conf. Proc. 714: X-ray Timing 2003: Rossi and Beyond, 714, 127

Distefano, C., Guetta, D., Waxman, E., & Levinson, A. 2002, ApJ, 575, 378

Doxsey, R. et al. 1977, IAU Circ., 3113

Emelyanov, A. N., Aleksandrovich, N. L., & Sunyaev, R. A. 2000, Astronomy Letters, 26, 297

Fender, R., Garrington, S. T., McKay, D. J., Muxlow, T. W. B., Pooley, G. G., Spencer, R. E., Stirling, A. M., Waltman, E. B. 1999, MNRAS, 1999, 304, 865

Fender R.P. 2004, in Compact Stellar X-ray sources, eds. W. H. G. Lewin & M. van der Klis, (Cambridge: Cambridge University Press), in press, astro-ph/0303339

Fender, R. P., Belloni, T. M., & Gallo, E. 2004, MNRAS, 355, 1105

Fomalont, E. B., Geldzahler, B. J., & Bradshaw, C. F. 2001a, ApJ, 558, 283

Fomalont, E. B., Geldzahler, B. J., & Bradshaw, C. F. 2001b, ApJ, 553, L27

Freeman, P. E., Kashyap, V., Rosner, R., & Lamb, D. Q. 2002, ApJS, 138, 185

Gallo, E., Corbel, S., Fender, R. P., Maccarone, T. J., & Tzioumis, A. K. 2004, MNRAS, 347, L52

Garcia, M. R., McClintock, J. E., Narayan, R., Callanan, P., Barret, D., & Murray, S. S. 2001, ApJ, 553, L47

Heinz, S. & Sunyaev, R. 2002, A&A, 390, 751

Heinz, S. 2002, A&A, 388, L40

Homan, J., Miller, J.M., Wijnands, R., van der Klis, Belloni, T., Steeghs, D. & Lewin, W.H.G. 2005, ApJ, 623, 383

Kaaret, P., Corbel, S., Tomsick, J. A., Fender, R., Miller, J. M., Orosz, J. A., Tzioumis, A. K., & Wijnands, R. 2003, ApJ, 582, 945

Kaluzienski, L. J. & Holt, S. S. 1977, IAU Circ., 3099

Longair, M. S. 1994, Cambridge: Cambridge University Press, —c1994, 2nd ed.,

Miller, J.M., et al. 2005, ApJ, submitted, astro-ph/0406272

Remillard, R.A., McClintock, J.E., Orosz, J.A. & Levine, A.M. 2005, ApJ, submitted, astro-ph/0407025

Revnivtsev, M., Chernyakova, M., Capitanio, F., Westergaard, N. J., Shoenfelder, V., Gehrels, N., & Winkler, C. 2003, The Astronomer's Telegram, 132

Reynolds, A. P., Parmar, A. N., Hakala, P. J., Pollock, A. M. T., Williams, O. R., Peacock, A., & Taylor, B. G. 1999, A&AS, 134, 287

Rupen, M. P., Mioduszewski, A. J., & Dhawan, V. 2003a, The Astronomer's Telegram, 137

Rupen, M. P., Mioduszewski, A. J., & Dhawan, V. 2003b, The Astronomer's Telegram, 142

Rupen, M. P., Mioduszewski, A. J., & Dhawan, V. 2004, The Astronomer's Telegram, 314

Sams, B. J., Eckart, A., & Sunyaev, R. 1996, Nature, 382, 47

Sault R.J. & Killeen N.E.B. 1998, The Miriad User's Guide, Sydney: Australia Telescope National Facility

Swank, J. 2004, The Astronomer's Telegram, 301

Tomsick, J. A., Corbel, S., Fender, R., Miller, J. M., Orosz, J. A., Tzioumis, T., Wijnands, R., & Kaaret, P. 2003a, ApJ, 582, 933

Tomsick, J. A., et al. 2003b, ApJ, 597, L133

Tomsick, J. A. & Kalemci, E. 2003, The Astronomer's Telegram, 198

Wachter, K, Leach, R, & Kellog E. 1979, ApJ, 230, 274

Wang, X. Y., Dai, Z. G., & Lu, T. 2003, ApJ, 592, 347

Weisskopf, M. C., Brinkman, B., Canizares, C., Garmire, G., Murray, S., & Van Speybroeck, L. P. 2002, PASP, 114, 1

White, N. E., & Marshall, F. E. 1983, IAU Circ., 3806

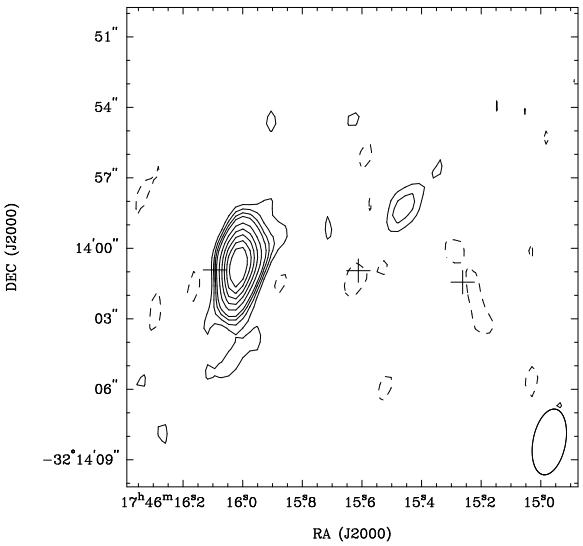

Fig. 1.— ATCA radio map at 8.64 GHz of the field near the black hole candidate H 1743−322 on 20 December 2003. The crosses (size of 1″) indicate the location of H 1743−322 (center), the eastern and western jets, as observed during the first *Chandra* observations two months later (on 12 February 2004). Contours are plotted at -2, 2, 3, 4, 5, 7, 9, 11, 13, 15, 18, 21, 25 and 30 times the r.m.s. noise level of 0.07 mJy beam^{-1}. The synthesized beam (in the lower right corner) is 2.8 × 1.4 arcsec^2, with the major axis at a position angle of –10.9 °.

This 2-column preprint was prepared with the AAS LaTeX macros v5.2.

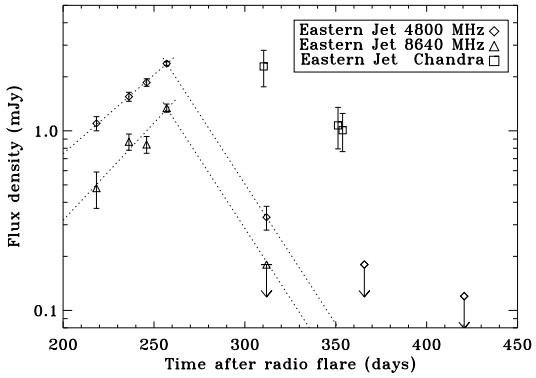

Fig. 2.— Radio light-curve at 8.6 GHz (3 cm) and 4.8 GHz (6 cm) of the eastern jet of H 1743−322 as measured by ATCA. Upper limits are plotted at the three sigma level. The dotted lines illustrate the exponential fit to the rise and decay of radio emission. The *Chandra* 0.3–8 keV unabsorbed flux (times 10^6) of the eastern jet is also plotted and this indicates the dates of the X-ray observations. The x-axis is the time since the major radio flare as observed by the VLA on 2003 April 8 (MJD 52738) by Rupen et al. 2003b.

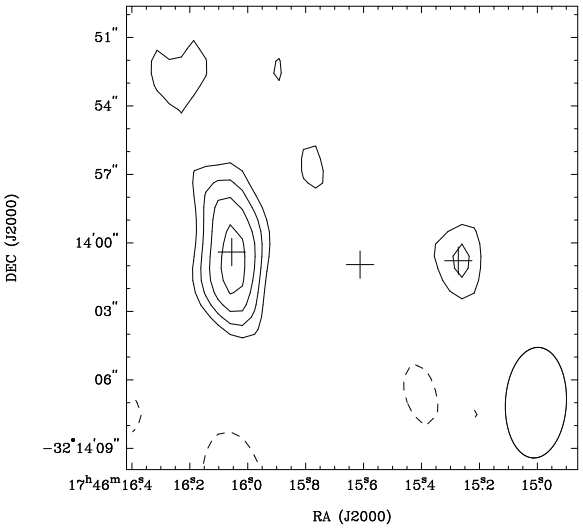

Fig. 3.— ATCA radio map at 4.8 GHz of the field near the black hole candidate H 1743−322 on 13 February 2004. The crosses indicate the location of H 1743−322 (center), the eastern and western jets. The weak source at the position of the western jet is consistent with location the X-ray counterpart. Contours are plotted at -2, 2, 3, 4, 5 times the r.m.s. noise level of 0.05 mJy beam^{-1}. The synthesized beam (in the lower right corner) is 4.8 × 2.7 arcsec^2, with the major axis at a position angle of –3.0 °.

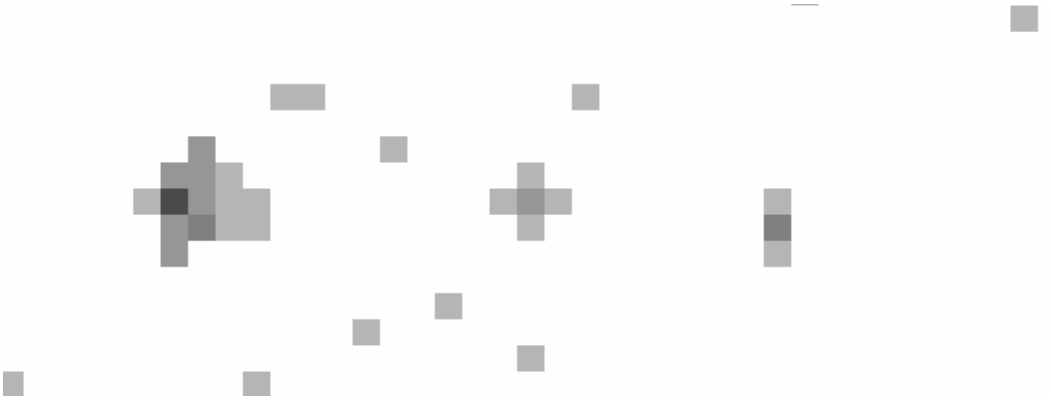

2004 February 12

2004 March 24

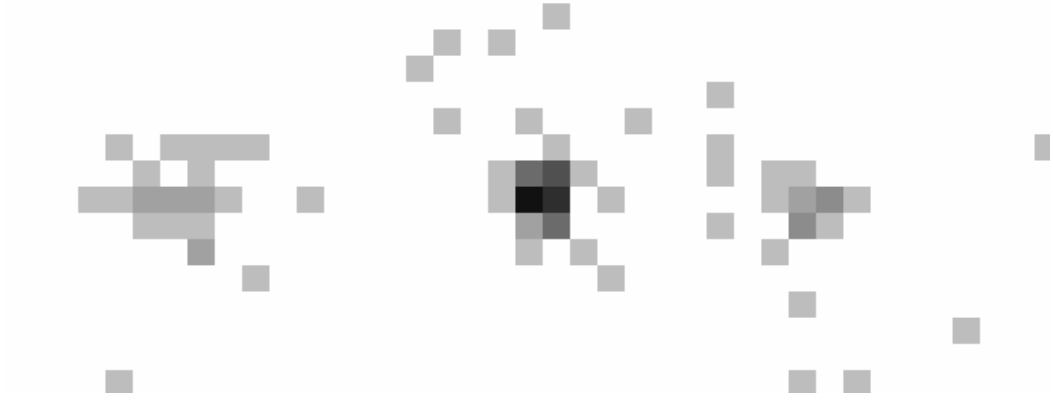

2004 March 27

Fig. 4.— X-ray images of H 1743−322 for the 0.3–8 keV band taken on 2004 February 12, March 24 and March 27. The grey level represents the number of X-ray counts per pixel with a maximal of respectively 6, 5, 13 counts on resp. 2004 February 12, March 24 and March 27. H 1743−322 is located at the center of the image, whereas the eastern jet is on the left and the western jet is on the right.

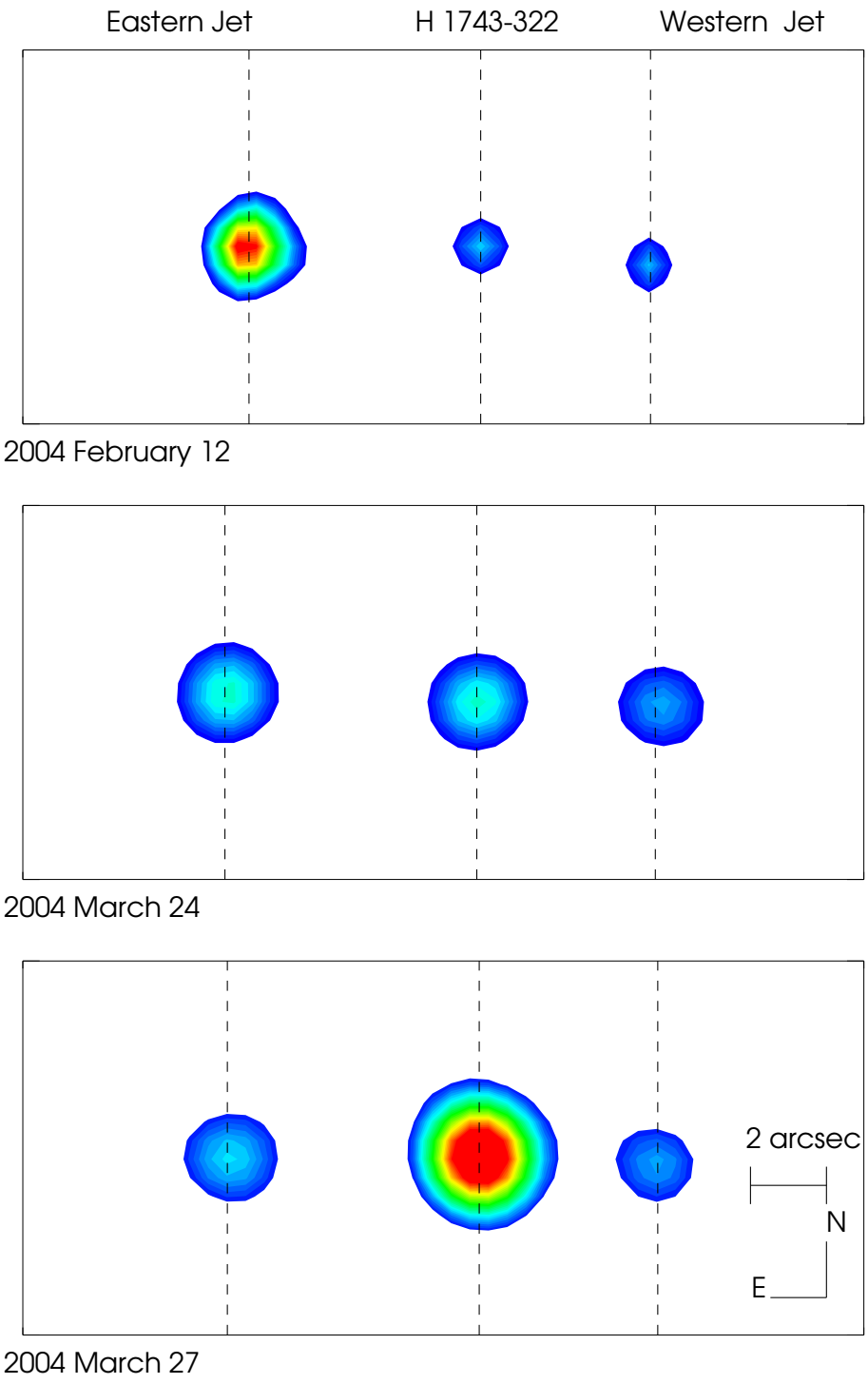

Fig. 5.— Filled contour plots produced by convolving the 0.3–8 keV images shown in Fig. 4 with a two-dimensional Gaussian with a width of two pixels in both directions. The vertical lines indicate the position of the X-ray sources in each observation. Each count image has been normalized by its integration time.

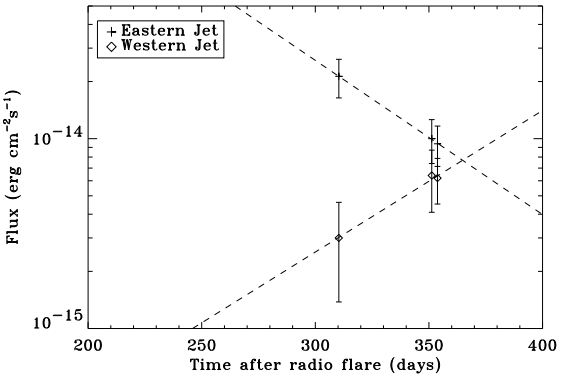

Fig. 6.— X-ray flux of the eastern (plus) and western (diamond) jets versus the time after the bright radio flare on 2003 April 8. The curves are the exponential decay (eastern jet) and "rise" (western jet) described in the text.

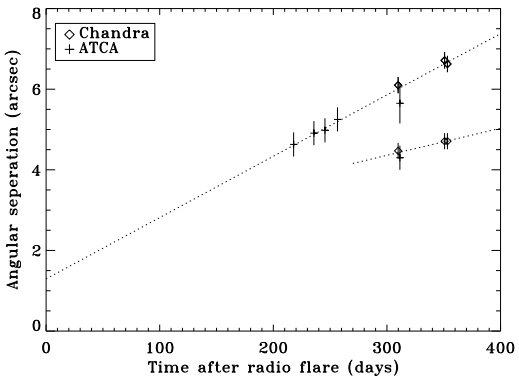

Fig. 8.— Angular separation between the BHC H 1743−322 and each jet versus time since the bright radio flare observed on 2003 April 8. This plot is based on ATCA (plus sign) and *Chandra* (diamond) data. The western jet is the one that is mowing slower. The dotted lines represent the linear fit to the proper motion of the jets assuming no deceleration.

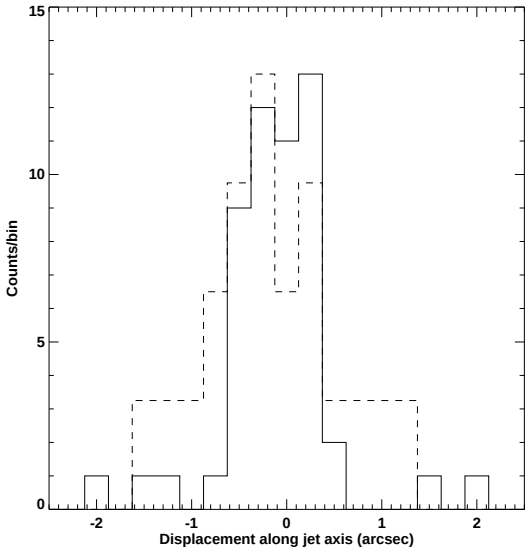

Fig. 7.— Distribution of the X-ray counts along the jet axis combining *Chandra* observations # 2 and 3. The dashed line is the profile of the eastern jet and the solid line is for H 1743−322 rescaled to match the peak of emission of the eastern jet. The bin size is 0.25 ″.

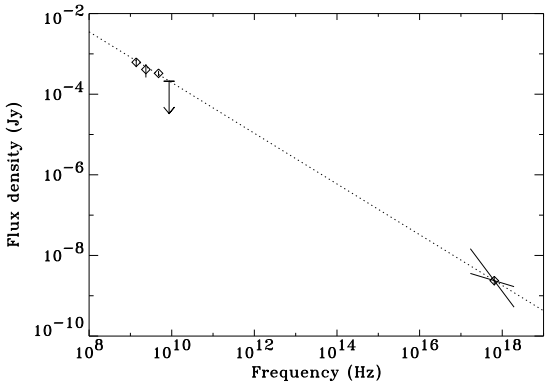

Fig. 9.— Spectral energy distribution of the eastern jet on 2004 February 13 as observed by ATCA and *Chandra*. The "bow tie" represents the *Chandra* constraints on the flux and spectral index of the X-ray emission. The spectral index error lines are at 90% confidence level with the column density frozen to value measured for the black hole H 1743−322.